9th AUSTRALASIAN
FLUID MECHANICS CONFERENCE,
AUCKLAND, 8-12 DECEMBER 1986

The Difficulties in the Measurements of Reynolds Stresses in Smooth- and in Rough-Wall Turbulent Boundary Layers

J. D. LI, S. M. HENBEST and A. E. PERRY

Department of Mechanical Engineering, University of Melbourne, Australia.
University of Melbourne, Australia.

1. INTRODUCTION

In this paper we attempt to obtain reliable hot-wire anemometry measurements of the Reynolds stresses over smooth and over "d-type" rough walls (see Perry, Schofield & Joubert 1969) with zero streamwise pressure gradients. In previous work (Perry, Lim & Henbest 1986), the non-dimensional stresses $\overline{w^2}/U_\tau^2$ and $\overline{uw}/U_\tau^2$ were found to be most difficult to measure reliably, ($\overline{v^2}/U_\tau^2$ has yet to be investigated in detail). Here, u, v and w are the streamwise, spanwise and normal fluctuating components of velocity respectively, and U_τ is the wall shear velocity. In the present work on the smooth wall we found that the Reynolds shear stress, $\overline{uw}/U_\tau^2$, measured in the mean-flow logarithmic law-of-the-wall region never exceeded 0.92 for the low R_θ value (4200) investigated here, (using U_τ obtained from the Clauser chart and the Preston tube methods). Here, R_θ is the Reynolds number based on the momentum thickness, θ, and the free stream velocity, $\overline{U_1}$. Past results at the University of Melbourne (Lim 1985, Erm et.al. 1986) at similar R_θ's gave similar results, whereas at higher R_θ's (>5000) gave values close to 1.0 in this region. On "d-type" rough walls, a reliable mean flow similarity method for determining U_τ needs to be developed. Nevertheless, using the Hama velocity defect law method (see Perry et.al. 1983) and momentum integral methods the estimates of U_τ obtained were considerably above the value expected from the "d-type" roughness $\overline{uw}$ plot.

When using X-wires in turbulent boundary layers some of the problems that may arise that could explain these discrepancies are: (1) thermal prong effect, which affects the frequency response of the wire (see Perry, Smits & Chong 1979); (2) hot-wire filament bowing; (3) probe misalignment; (4) excessive cone angles of the approaching velocity vectors (see Perry et.al. 1983); (5) aerodynamic prong effects and (6) spatial resolution. Each of these possibilities were investigated in turn by: (1) operating the same set of X-wires at different resistance ratios; (2) using different sets of X-wires and checking the hot-wire filaments; (3) checking for probe misalignment; (4) "flying" the wires to reduce the cone angles, using the "flying hot-wire" apparatus as described by Watmuff et. al. (1983); (5) using two different probe-prong geometries and (6) using sets of X-wires with different wire lengths (but unfortunately we have not used different wire spacings); and it was found that the same $\overline{uw}/U_\tau^2$ profiles were obtained to within ±3%. Lim (1985) did use different wire spacings and found that $\overline{uw}$ did not change a detectable amount. Given these facts we tentatively believe that the measured Reynolds shear-stress profiles are correct and that the standard extrapolation procedure based on the assumption that the total shear stress is invariant with z (the distance normal from the wall) in the logarithmic region needs to be revised.

All hot-wire anemometry techniques used here are as in Perry, Henbest & Chong (1986).

2. WHAT IS THE EXPECTED SHEAR STRESS DISTRIBUTION IN TURBULENT BOUNDARY LAYER FLOWS?

Most workers assume that the total shear stress distribution (turbulent plus viscous) is invariant with z in the logarithmic wall region in flat plate boundary layer flows. i.e.

$$\frac{\tau}{\rho U_\tau^2} = \frac{-\overline{uw}}{U_\tau^2} + \frac{\nu}{U_\tau^2}\frac{d\overline{U}}{dz} = 1 \qquad (1),$$

where τ is the total shear stress, ρ is the fluid density, $\overline{U}$ is the mean velocity a distance z from the wall and ν is the kinematic fluid viscosity. Such a constant total shear stress distribution is only an approximation and the true variation must include the mean flow inertia effects. Perry (1968) carried out an analysis for the total shear stress distribution in the so called "equilibrium" turbulent boundary layers by assuming that (1) the law of the wall and (2) the velocity defect law are valid, and by using the momentum integral and continuity equations was able to deduce the total shear stress distribution, $\tau/\rho U_\tau^2$, as a function of η and ω, where $\eta=z/\Delta$, $\omega=\sqrt{(2/C_f')}$. Here, Δ is an integral boundary layer thickness and C_f' is the usual local skin friction coefficient. The relevant part of this work to the present measurements is the application of the analysis to zero pressure gradient smooth wall boundary layers and to "d-type" roughness development. In the case of smooth walls it can be shown that

$$\frac{\tau}{\rho U_\tau^2} = 1 - f(\eta,\omega) \qquad (2)$$

and in the logarithmic region we have

$$\left.\begin{array}{l} \text{for } \omega = O(10), \quad f(\eta,\omega) = 0 \\ \text{and for } \omega \to \infty, \quad f(\eta,\omega) = \eta/(\kappa C_1) + \text{----}. \end{array}\right\} \qquad (3).$$

Here, κ is the Kármán constant and $C_1 = \int_0^\infty D(\eta)\,d\eta$, where $D(\eta)$ is the velocity defect law. Hama (1954) assumed that $D(\eta)$ was of the form

$$D(\eta) = \frac{\overline{U_1} - \overline{U}}{U_\tau} = -\frac{1}{\kappa}\ln(\eta) + B \;; \quad 0 < \eta \le .15 \qquad (4a)$$

$$= 9.6(1-\eta)^3 \;; \quad .15 < \eta \le 1.0 \qquad (4b)$$

where B=2.309. This gives C_1=3.3715. The integral boundary layer thickness length scale, Δ, is defined by $\Delta=(\omega\delta^*)/C_1$, where δ^* is the displacement thickness. Equation (2) is shown in figure 1 for the above two cases. Also shown are the wall asyptotes given by equation (3). As $\omega\to\infty$, all Reynolds shear stress profiles should collapse onto a universal curve. Thus showing that for $\omega\to\infty$ true equilibrium is achieved, i.e. we have self preserving distributions of both $D(\eta)$ and $\tau/\rho U_\tau^2$.

For R_θ less than 5000 the velocity defect law should really be expressed as $D=D(\eta,\omega)$, (eg: see

Coles 1968), in which case, the total shear stress profiles shown in figure 1 may not be applicable. There are two extreme cases which we could consider: (1) a self preserving defect law in combination with the law of the wall or (2) a self preserving Reynolds shear stress profile in combination with the law of the wall. Both results should lead to self preserving flow in both defect and total shear stress distributions at $\omega \to \infty$. At moderate Reynolds numbers, we believe the development of the layer might be somewhere between these two cases. Therefore, we might expect the Reynolds shear stress data measured in the logarithmic region to fall somewhere between the two limiting profiles given by

$$\frac{-\overline{uw}}{U_\tau^2} = 1 - \frac{1}{\kappa \eta K_\tau} \quad ; \quad \omega = O(10) \qquad (5a)$$

$$\frac{-\overline{uw}}{U_\tau^2} = 1 - \frac{\eta}{\kappa C_1} - \frac{1}{\kappa \eta K_\tau} \quad ; \quad \omega \to \infty \qquad (5b)$$

where $K_\tau = \Delta U_\tau / \nu$ is called the Kármán number. Here the viscous contribution to the total stress has been formulated using (4a).

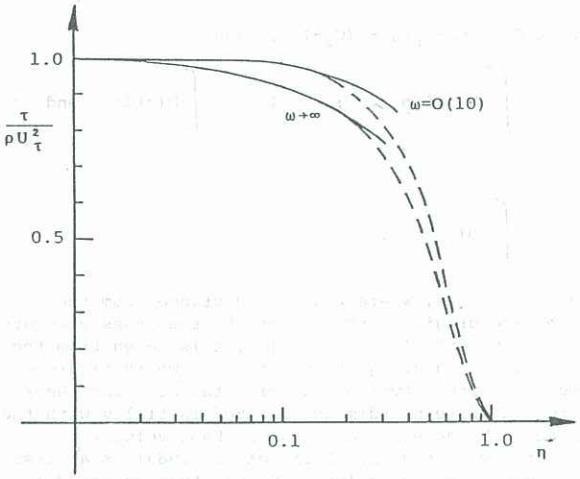

Figure 1. Distribution of $\tau/\rho U_\tau^2$ versus η for $\omega \to \infty$ and $\omega = O(10)$. Solid lines are the wall asymptotes given by equation (3) for a smooth wall.

3. SMOOTH WALL EXPERIMENTAL RESULTS.

All smooth wall broad-band turbulence measurements reported here were taken 3000 mm from the trip wire and at a free stream velocity of 10 m/s. This corresponded to an R_θ of 4200.

Figure 2 shows a typical smooth wall $\overline{uw}/U_\tau^2$ experimental profile together with the distributions given by equation (5a) and (5b). This figure shows how large the region of uncertainty (shown shaded) is when attempting to extrapolate smooth wall $\overline{uw}$ data to the wall with our present knowledge of turbulent boundary layers. This region of uncertainty may even be larger than shown in figure 2. It appears that the appropriate extrapolation law might be (5b), although there is no firm theoretical reason why it should be. In fact, at higher R_θ (>5000), results of Lim and Erm et.al. show that equation (5a) is more applicable. The Reynolds shear stress results in figure 2 are slightly below that given by equation (5b). We checked that reasons (1),(2),(3),(4) and (5) listed above were not the cause. Spatial resolution (reason 6) was checked by reducing the length of the wires from 1.00mm to 0.5mm and no detectable change in Reynolds shear stress was measured. However, a noticeable change in $\overline{w^2}$ was measured as seen in figure 3, hence spatial resolution could still be a problem for this quantity. A possible explanation for this is given later. The smooth wall $d\theta/dx$ value for U_τ agreed well with the Clauser chart and Preston tube values. Here x is the streamwise distance. This is suprising, since secondary flow is known to have a strong influence (although we know that secondary flow

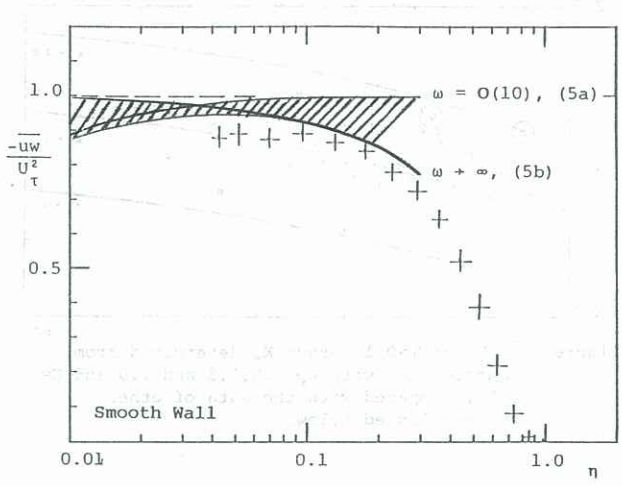

Figure 2. Measured $\overline{uw}/U_\tau^2$ distribution on the smooth wall together with the distributions given by equations (5a) and (5b).

was small) and there is the uncertainty associated with finding the local deriviative of a curve defined by a set of discrete data points.

We believe that the value of U_τ is correct since the Clauser and Preston tube techniques are universally accepted. Figure 3 shows the $\overline{w^2}/U_\tau^2$ results measured with different probes and with different resistance ratios for a given probe and with the X-wires stationary and with the X-wires flying. Perry, Henbest & Chong (1986) showed that in the logarithmic wall region that the distribution of $\overline{w^2}/U_\tau^2$ is expected to follow

$$\frac{\overline{w^2}}{U_\tau^2} = A_3 - \frac{4}{3} C (\eta)^{-\frac{1}{2}} (K_\tau)^{-\frac{1}{2}} \qquad (6)$$

where A_3 and C are universal constants. Perry, Henbest & Chong determined the value of C, from their experimental streamwise spectral measurements, to be 6.08. Perry, Lim & Henbest (1986) determined the value of A_3 by plotting curves of $\overline{w^2}/U_\tau^2$ at η=0.1 versus K_τ for various values of A_3 and correlating these curves with their data and the data of other workers. This is shown in figure 4. The smooth wall broad-band results of Perry, Lim & Henbest corresponded to a value of A_3=1.6. When they included the data of other workers they estimated the value of A_3 to be 1.5. However, as can be seen in the figure there is considerable scatter and this shows the difficulty other workers are also having in obtaining reliable results; since by dimensional analysis alone results from a given flow geometry (ie. a boundary layer

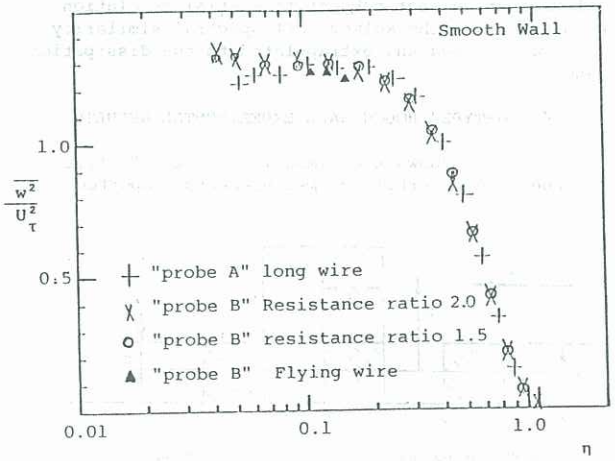

Figure 3. Measured $\overline{w^2}/U_\tau^2$ distribution on the smooth wall for the cases listed.

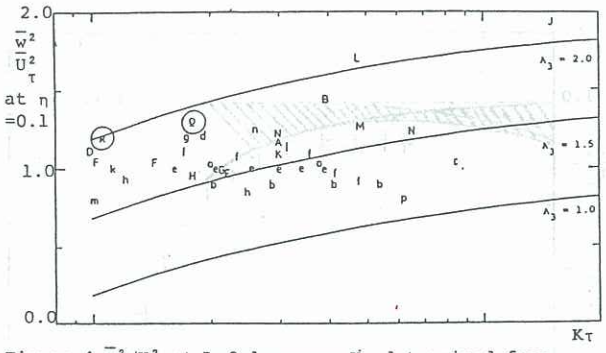

Figure 4 $\overline{w^2}/U_\tau^2$ at η=0.1 versus K_τ determined from equation (6) with A_3= 1.0,1.5 and 2.0 and C= 6.08, compared with the data of other workers listed below.

Smooth Wall Boundary Layers

B Andreopoulos & Bradshaw 1981
D Antonia & Luxton 1971
F Erm, Smits & Joubert 1986
G Gupta & Kaplan 1972
H Hancock & Bradshaw 1983
I Klebanoff 1954
K Murlis, Tsai & Bradshaw 1982
L Willmarth & Bogar 1977
M Perry, Lim & Henbest 1986
Q Present results

Rough Wall Boundary Layers

A Acharya & Escudier 1984
C Andreopoulos & Bradshaw 1981
E Antonia & Luxton 1971
J Mulhearn 1978 (very rough)
N Perry, Lim & Henbest 1986
R Present results (d-type)

Smooth Pipes & Ducts

a Abell 1974
d Bremhorst & Walker 1973
e Henbest 1983
g Hooper & Harris 1982
h Hunt & Joubert 1979
k Laufer 1954
m Lawn 1971
n Sabot & Comte-Bellot 1976

Rough Pipes

b Abell 1974
f Henbest 1983
p Sabot, Saleh & Comte-Bellot 1977

or pipe) should collapse to a universal curve. The present smooth wall results are more consistent than the previous measurements since they passed checks (1) though to (5). There is some doubt concerning spatial resolution since this check failed, as noted earlier, even though the Reynolds shear stress profiles appeared to be insensitive to this effect. This could be due to $\overline{w^2}$ having an extensive Kolmogoroff (1941) inertial-subrange, whereas the cross-power spectral density of $\overline{uw}$ probably does not have significant contribution from the inertial-subrange. Nevertheless, the data here give a value of A_3=1.90 and it will be seen later that this value agrees with the value obtained from the "d-type" rough wall results using the same techniques and checks. Perry, Lim & Henbest (1986) found from their assumed spectral similarity laws that A_3=1.90. This calculation was not subject to spatial resolution problems since the Kolmogoroff spectral similarity law was assumed and extrapolated to the dissipation range.

4. "d-TYPE" ROUGH WALL EXPERIMENTAL RESULTS.

Figure 5 shows the dimensions of the "d-type" roughness. All turbulence measurements reported here were taken 2640 mm from the leading edge and at a free stream velocity of 5 m/s.

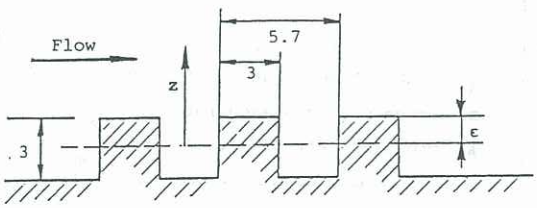

Figure 5. Dimensions of the "d-type" roughness (in mm) and definition of the effective origin.

A particular characteristic of "d-type" roughness is that C_f' is constant with x. This was found to be the case from the linear development of θ with x. This property makes the determination of $d\theta/dx$ more precise. Also, the velocity defect law was found to be valid since all data collapsed very well on a $\overline{U}/\overline{U_1} = f(z/\delta^*)$ plot and this is consistent with a self preserving defect law and a constant C_f'. In fact, this case corresponds to Rotta's (1962) precise equilibrium flow and is the only known case. Hence, the shear stress distribution must also be self preserving as the analysis of Perry shows. Because of these facts there should be no uncertainty in how the shear stress should behave in the logarithmic region. The analysis for "d-type"roughness is quite different theoretically from the smooth wall analysis because C_f' is constant. Using the analysis of Perry, the result for "d-type" roughness can be shown to be

$$\frac{-\overline{uw}}{U_\tau^2} = 1 - \frac{\eta}{G}\left(\frac{\omega}{\kappa} - \frac{B}{\kappa} - \frac{2}{\kappa^2} + \frac{\ln(\eta)}{\kappa^2}\right) - \frac{1}{\kappa\eta K_\tau} \qquad (7)$$

where $G = (C_1 - I_1)\omega - (C_2 - I_2)$, and

$$C_2 = \int_0^\infty D(\eta)^2 d\eta \quad ; \quad I_1 = \int_0^{\eta_0} D(\eta) d\eta \quad \text{and}$$

$$I_2 = \int_0^{\eta_0} D(\eta)^2 d\eta \ .$$

Here, $\eta_0 = \varepsilon/\Delta$, where ε is the distance from the effective origin to the top of the roughness elements (see figure 5). In equation (7), z is taken from the effective origin. Equation (7) is shown in figure 6 together with a typical experimental Reynolds shear stress profile non-dimensionalized initially with the value of U_τ determined using the Hama velocity defect law method (see Perry et.al. 1983) as a first approximation. The value of U_τ was then adjusted so that the Reynolds shear stress profile in the logarithmic region fitted the line given by equation (7). The value of U_τ^2 obtained in this manner agreed very well with the $d\theta/dx$ value and was within 10% of the Hama velocity defect law value. Here we have a self-preserving velocity defect distribution but it is slightly different from the Hama law. We believe that the use of this extrapolation method is a reasonably reliable method of estimating U_τ on "d-type" roughness. On the "d-type" roughness the cone angle relative to a stationary observer measured in the uw-plane with a stationary X-wire and with a flying X-wire were found to be the same and small. Therefore, no cone angle problem existed.

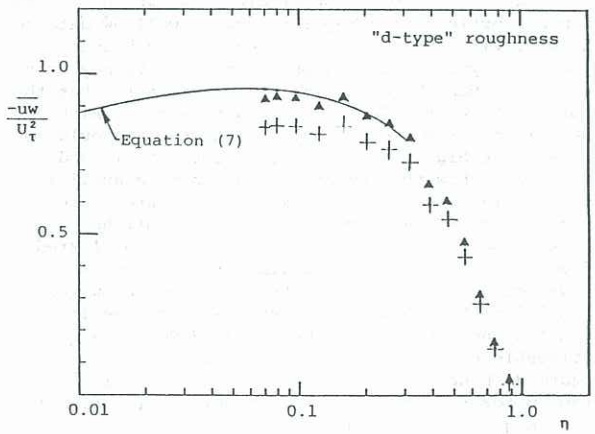

Figure 6. Measured distribution of $\overline{uw}$ on the "d-type" roughness non-dimensionalized with Hama U_τ (+) and with the Reynolds shear stress extrapolation scheme U_τ (▲).

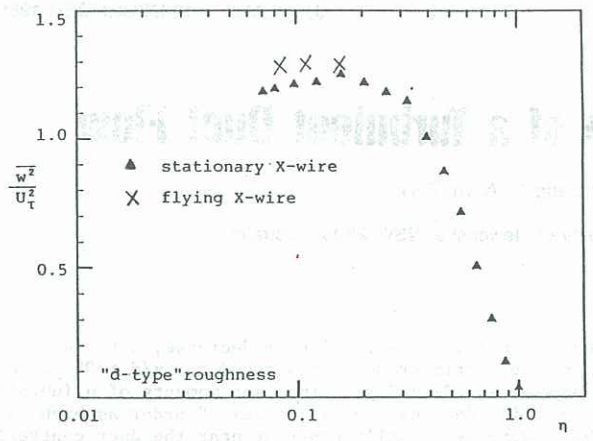

Figure 7. $\overline{w^2}/U_\tau^2$ distribution on the "d-type" roughness. U_τ determined from the Reynolds shear stress extrapolation method.

Since we now have a 'reliable' estimate of U_τ, values of $\overline{w^2}/U_\tau^2$ can be plotted and compared with equation (6). Figure 7 shows the $\overline{w^2}/U_\tau^2$ results for the "d-type" roughness. For these results none of the redundancy checks have been done except for (5) at the time of writing. These results give a value of A_3 = 1.95 as shown in figure 4. This value is close to the smooth wall value of 1.90.

5. A NOTE ABOUT "k-TYPE" ROUGHNESS

Perry (1968) showed that for "k-type" roughness and for ω=O(10) the appropriate shear stress distribution is given by equation (5a). Lim (1985) obtained a self-preserving defect law on "k-type" roughness when he used values of U_τ obtained by extrapolating the measured Reynolds shear stress profiles with equation (5a). Thus, the initial hypothesis in the analysis, of a self preserving defect law, was upheld. On the "k-type" roughness studied by Lim there was a cone angle problem and it was necessary to use X-wires with an inclued angle of 120 degrees (and this was checked by flying the wires) to obtain an accurate estimate of the Reynolds shear stress and hence U_τ. The reason for the cone angle problem with the "k-type" roughness discussed here is that a large Hama (1954) roughness function occurred, whereas for the "d-type" roughness this function was small (see Perry et.al. 1983).

6. CONCLUSIONS & DISCUSSION

In all turbulence work which is attempting to verify broad-band turbulence similarity laws (see Perry, Henbest & Chong 1986), it is necessary to obtain accurate measurements of the Reynolds stresses and estimates of the wall shear velocity. In this work we have endeavoured to do this by incorporating many redundancy checks into our smooth wall X-wire measurements. We have also developed a method of estimating the wall shear velocity on "d-type" roughness, which relies on an extrapolation of the measured Reynolds shear stress profile to the wall assuming that the layer is a "self preserving equilibrium boundary layer". The value of wall shear velocity obtained agrees well with the value obtained using the momentum integral method. The results so far for the smooth wall and for the "d-type" roughness give values of A_3 (a universal constant related to the normal turbulence intensity similarity law in the logarithmic region) which are consistent with each other and are further verified by the spectral results and analysis of Perry, Lim & Henbest (1986).

This work is in its initial stages and further work is necessary over a wide range of Reynolds numbers before verification of this or any other similarity law is possible.

The authors wish to thank the Australian Research Grants Scheme for the financial support of this project.

7. REFERENCES

Abell, C.J. 1974 Ph.D.Thesis, University of Melbourne, Australia.
Acharya, M.E. & Escudier, M.P. 1984 BBC Brown Boveri and Co. Ltd., Report KLR 84-179C.
Andreopoulos, J. & Bradshaw, P. 1981 Boundary Layer Meteorology, Vol. 20, 201-213.
Antonia, R.A. & Luxton, R.E. 1971 J. Fluid Mech., Vol. 48, 721-701.
Bremhorst, K. & Walker, T.B. 1973 J.Fluid Mech., Vol. 61, 173-186.
Coles, D.E. 1968 Proc. Computation of Turbulent Boundary Layers, Stanford.
Erm, L.P., Smits, A.J. & Joubert, P.N. 1986 Turbulent Shear Flows V, Springer-Verlag.
Gupta, A.K. & Kaplan, R.E. 1972 Phys. Fluids, Vol. 15, 981-985.
Hama, F.R. 1954 Trans SNAME, Vol. 62.
Hancock, P.E. & Bradshaw, P. 1983 Trans ASME, Vol. 105, 284-289.
Henbest, S.M. 1983 Ph.D. Thesis, University of Melbourne, Australia.
Hooper, J.D. & Harris, R.W. 1982 Aust. Atomic Energy Commission Report No. E516.
Hunt, I.A. & Joubert, P.N. 1979 J. Fluid Mech., Vol. 133, 83-112.
Klebanoff, P.S. 1954 NACA TN 3178.
Kolmogoroff, A.N. 1941 C.R. Sci. URSS, Vol.30, 301-305.
Laufer, J. 1954 NACA Report 1174.
Lawn, C.J. 1971 J. Fluid Mech., Vol. 48, 477-505.
Lim, K.L. 1985 Ph.D. Thesis, University of Melbourne, Australia.
Mulhearn, P.J. 1978 Phys. Fluids, Vol. 21, 1113-1115.
Murlis, J., Tsai, H.M. & Bradshaw, P. 1982 J. Fluid Mech., Vol. 122, 13-56.
Perry, A.E. 1968 "Equilibrium boundary layers" Unpublished.
Perry, A.E., Schofield, W.H. & Joubert, P.N. 1969 J. Fluid Mech., Vol. 37, 383-413.
Perry, A.E., Smits, A.J. & Chong, M.S. 1979 J. Fluid Mech., Vol. 90, 415-431.
Perry, A.E., Lim, K.L., Henbest, S.M. & Chong, M.S. 1983 Fourth Symposium on Turbulent Shear Flows, Karlsruhe, Germany.
Perry, A.E., Henbest, S.M. & Chong, M.S. 1986 J. Fluid Mech., Vol. 165, 163-199.
Perry, A.E., Lim, K.L. & Henbest, S.M. 1986 "An Experimental Study of the turbulent structure in smooth- and rough-wall boundary layers", in preparation.
Rotta, J.C. 1962 Progress in Aero. Sci., Vol. 2, Permagon Press.
Sabot, J. & Comte-Bellot, G. 1976 J. Fluid Mech., Vol. 74, 767-796.
Sabot, J., Saleh, I. & Comte-Bellot, G. 1977 Phys. Fluids, Vol. 20, S150-S155.
Watmuff, J.H., Perry, A.E. & Chong, M.S. 1983 Experiments in Fluids, Vol. 1, 63-71.
Willmarth, W.W. & Bogar, T.J. 1977 Phys. Fluids, Vol 20, S9-S21.